JOURNAL OF APPLIED ELECTROCHEMISTRY 18 (1988) 459–462

Mono- and multilayer formation studies on silver anodic film formation of silver bromide

S. JAYA, T. PRASADA RAO*, G. PRABHAKARA RAO

Central Electrochemical Research Institute, Karaikudi 623 006, India

Received 31 March 1987; revised 16 November 1987

The mono- and multilayer formation of silver bromide on silver was investigated by cyclic voltammetric and single potential step current–time transient experiments at different concentrations of bromide. A monolayer peak was noticed at potentials more negative than the Ag/AgBr reversible potential. The electrodeposition of AgBr was shown to occur by adorption–desorption and nucleation–growth kinetic processes during mono- and multilayer formation, respectively.

1. Introduction

The widespread use of silver halides (AgX) as reference electrodes [1], ion-selective electrodes [2] and in photography [3], has led to a number of investigations of the anodic film formation of AgX on Ag. Most of these have been restricted to the multilayer formation of AgX and were obtained using galvanostatic and/or microscopic studies [4–8]. Recently, we have reported results for both the mono- and multilayer formation of Ag_2S [9], AgCl [10] and AgI [11] using cyclic voltammetric and single potential step current–time (i–t) transients. Nevertheless there are no reports concerning monolayer formation of AgBr on Ag, so the aim of the work was to elucidate the mechanism and kinetics of the growth of AgBr films by employing cyclic voltammetric and i–t transient studies.

2. Experimental details

Experiments were carried out using a Wenking potentiostat and Wenking scan generator (Model VSG 72). The working electrode was a polycrystalline silver disc ($A = 0.32\,cm^2$) embedded in Teflon. The auxiliary electrode was a platinum foil of large area $\sim 6\,cm^2$. The reference electrode was a normal calomel electrode with a Luggin probe positioned ~ 1 mm from the electrode surface.

Before each experiment the silver disc electrode was polished with emery papers of increasing fineness (1/0 to 4/0) and then rinsed with water, acetone, ethanol and water again. Solutions were flushed with N_2 before and during each experiment. Triple distilled water and A.R. grade chemicals were used. Experiments were conducted at 300 K.

3. Results and discussion

3.1. *Multilayer formation studies*

Figure 1 shows a few examples of cyclic voltammograms obtained in 10^{-1}, 10^{-2}, 10^{-3} and 10^{-4} M KBr (curves A, B, C and D, respectively) in aqueous 0.1 M $NaNO_3$ solutions during electrodeposition of AgBr on Ag. These triangular scans were reversed in the initial stages of multilayer formation of AgBr [12]. The main features of these curves are (1) a rapid rise in current during forward scan once nucleation begins; (2) an anodic current maximum on reverse scan; (3) a characteristic cross-over loop; and (4) a single cathodic reduction peak corresponding to the AgBr deposit formed at anodic potentials.

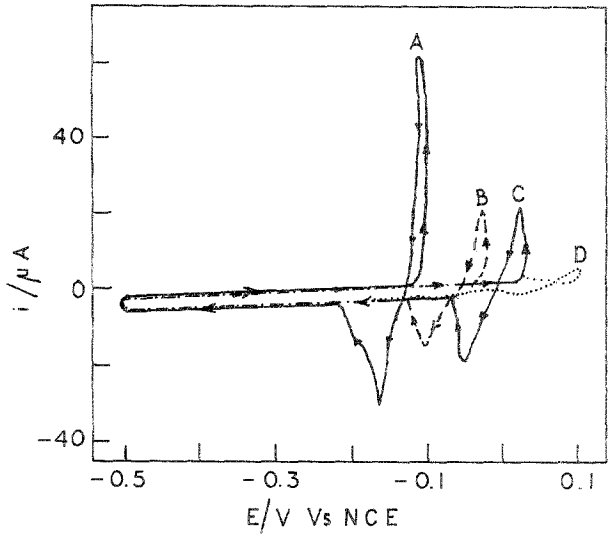

Fig. 1. Cyclic voltammetric curves obtained with polycrystalline silver disc electrode in x M KBr containing 0.1 M $NaNO_3$ as supporting electrolyte by reversing the triangular scan in initial stages of crystallization ($x = 10^{-1}$, 10^{-2}, 10^{-3} and 10^{-4} M for curves, A, B, C and D, respectively). Sweep rate = $30\,mV\,s^{-1}$.

These features indicate nucleation and subsequent grain growth processes [12]. Further, the charge associated with the nucleation and growth process is large (> 1 mC) so the process must be 3D rather than 2D. Moreover, on changing the sweep rate (Fig. 2), or potential limit of the triangular scan (Fig. 3), during the multilayer formation of AgBr on Ag from 10^{-3} M KBr solution, the cross-over potential remains con-

* Address of author to whom correspondence should be addressed: Regional Research Laboratory, Industrial Estate P.O., Trivandrum 695 019, India.

0021-891X/88 $03.00 + .12

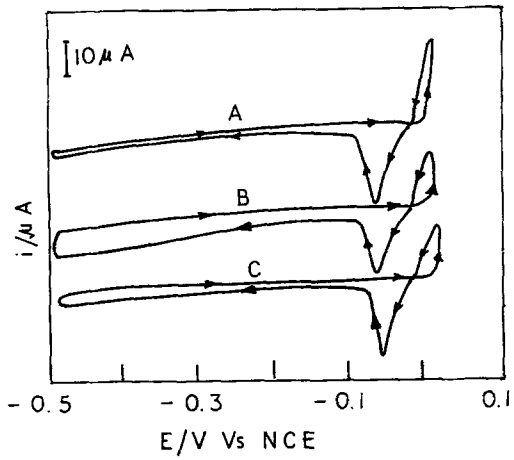

Fig. 2. Effect of sweep rate on the multilayer formation of AgBr from 10^{-3} M KBr in 0.1 M $NaNO_3$ solution onto Ag. Sweep rate = 6, 18 and 50 mV s^{-3} for curves A, B and C, respectively.

stant, thus indicating that the cross-over potential is indeed the Nernst reversible potential of the system [13]. Similar observations and conclusions were drawn by changing KBr concentration to 10^{-4}, 10^{-2}, 10^{-1} or 1 M. The Nernst reversible potentials obtained for different concentrations of KBr in aqueous 0.1 M $NaNO_3$ solutions are shown in curve A of Fig. 4 as a function of $p[Br^-]$. Curve B shows a plot of the theoretical Nernst reversible potentials [1] of Ag/AgBr electrode vs $p[Br^-]$ for which the thermodynamic relationship is given in Equation 1

$$E_r(\text{mV NHE}) = 0.071 - 0.059 \log [Br^-] \quad (1)$$

The experimental data of curve A of Fig. 4 can be expressed in the form of equation (2)

$$E_r(\text{mV NHE}) = 0.095 - 0.060 \log [Br^-] \quad (2)$$

The agreement between the two equations is reasonable. Nucleation–growth loops could not be resolved on decreasing the bromide concentration to 10^{-5} M in aqueous 0.1 M $NaNO_3$ solutions.

3.2. *Current–time transient studies*

Single step potentiostatic current–time (i–t) transients

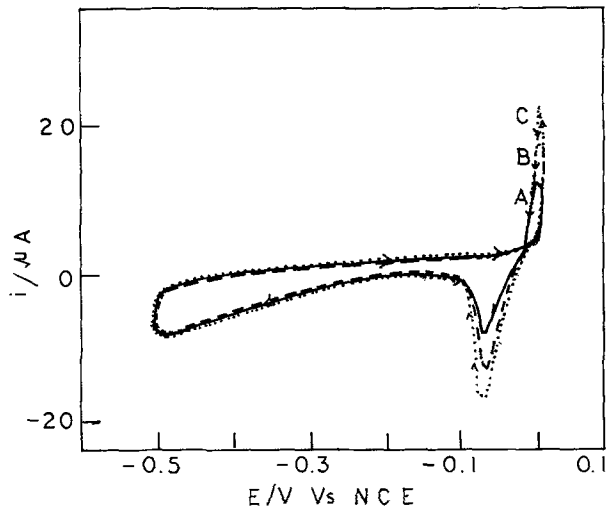

Fig. 3. Effect of varying the potential limit ($E(T)$) of triangular scans during the multilayer formation of AgBr from 10^{-3} M KBr in 0.1 M $NaNO_3$ solution onto Ag. $E(T)$ = 0.017, 0.020 and 0.022 V for curves A, B and C, respectively.

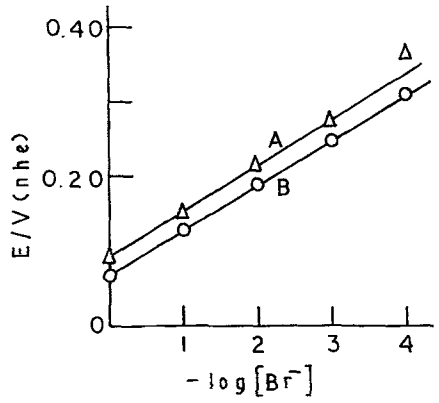

Fig. 4. Plot of Nernstian reversible potential as a function of KBr concentration. Curve A, experimental; curve B, theoretical.

obtained by stepping the potential from −0.5 to −0.056, 0.03 and 0.30 V vs NCE for 10^{-2}, 10^{-3} and 10^{-5} M KBr solutions (curves A, B and C, respectively) are shown in Fig. 5. From these it may be deduced that the anodic film formation of AgBr occurs by a nucleation/growth mechanism and not by a dissolution process [14, 15]. Rigorous analysis of the curves is difficult, however, because of the large double-layer charging current at short times and the dominance of semi-infinite linear diffusion at long times. Nevertheless, in the region of the rising part of the transients, the data are consistent with a time-dependent nucleation of bulk crystals coupled with their diffusion-controlled growth, for which the theoretical reponse is [16] $i(t) = Z\int_0^t N'(\tau)(t-\tau)^{1/2}d\tau$.

Here $N(t)$ is the number of crystals as a function of time, the superscript prime (as in $N'(\tau)$) indicates the first derivative with respect to time, and Z is a constant (at constant potential) given by [16]

$$Z = \pi nF(2DC_b)^{3/2}\varrho_m^{-1/2}\left(1 - \exp\left(\frac{-nF}{RT}\eta\right)^{3/2}\right)$$

Unfortunately, the poor resolution of the experimental $i(t)$ transients (*cf.* Fig. 6) does not allow the precise time dependence of $N(t)$ to be determined at the present time.

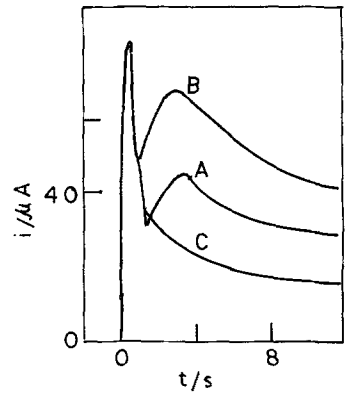

Fig. 5. Potentiostatic current–time transients obtained by stepping the potential from −0.5 V to −0.056, 0.03 and 0.30 V vs NCE (curves A, B and C, respectively) during multilayer formation of AgBr on silver from 10^{-2}, 10^{-3} and 10^{-5} M of KBr in aqueous 0.1 M $NaNO_3$ solution.

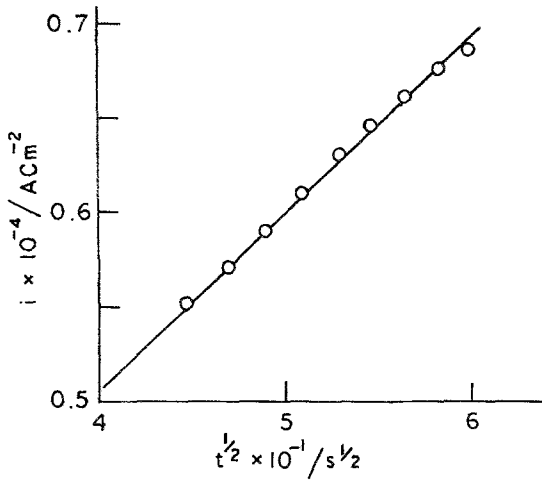

Fig. 6. Linear dependence between current and $t^{1/2}$ for the middle, rising section of the transient (curve B, Fig. 5).

3.3. *Monolayer formation studies*

Figure 7 shows a typical cyclic voltammogram obtained at a sweep rate of 100 mV s^{-1} in the potential scan range of −1.0 to −0.07 V vs NCE during electrodeposition of AgBr on Ag from 10^{-3} M KBr in aqueous 0.1 M $NaNO_3$. As is clear from Fig. 8, a single monolayer peak occurs at −0.17 V vs NCE (or 0.115 V vs NHE), much more positive to the reversible potential of Ag/AgBr in 10^{-3} M KBr solution, namely −0.01 V vs NHE. The corresponding cathodic peak occurs at −0.210 V vs NCE. The plot of anodic (curve A) and cathodic (curve B) peak currents (i_p) obtained at different sweep rates (v) gives a linear relationship (*cf.* Fig. 8) which indicates that the anodic peak at −0.17 V vs NCE is due to monolayer or sub-monolayer formation of AgBr on Ag. This is coroborated by the fact that the charge associated with the peak at −0.17 V vs NCE during anodic film formation of AgBr is found to be 6.7 μC cm^{-2}, much less than that required to form a crystalline monolayer.

The monolayer peaks were subjected to analysis according to the theoretical models suggested by Bosco and Rangarajan [18] to distinguish between nucleation–growth and adsorption–desorption kinetic process that are operative during monolayer formation. Thus on changing the sweep rate from 11 to

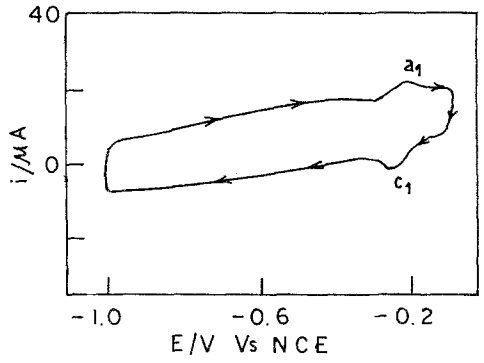

Fig. 7. Cyclic voltammograms obtained with polycrystalline silver disc electrode in 10^{-3} M KBr containing 0.1 M $NaNO_3$ as supporting electrolyte in the potential scan range −1.0 to −0.07 V vs NCE at a sweep rate of 100 mV s^{-1}.

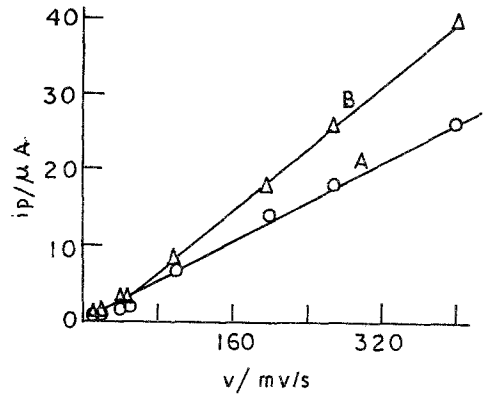

Fig. 8. Plot of monolayer peak currents with sweep rate. Curve A, anodic; curve B, cathodic.

400 mV s^{-1}, the peak width at half height ($\Delta E_{1/2}$) remains constant at 90 mV indicating that monolayer formation occurs by adsorption–desorption kinetic process (as $\Delta E_{1/2}$ is expected to vary from 0 to 60 mV on change of sweep rate from 0 to ∞ for either instantaneous or progressive nucleation growth. The anodic (E_{pa}) and cathodic (E_{pc}) peak potentials of monolayer formation and the difference between E_{pa} and E_{pc}, i.e. ΔE_p at various sweep rates are listed in Table 2. The peak potentials of a and c are symmetrical in the sweep rate range 11 to 40 mV s^{-1} indicating that the monolayer formation of AgBr is reversible. At sweep rates $\geqslant$ 40 mV s^{-1}, the E_{pa} and E_{pc} shift in the direction of potential scan expected for the irreversible monolayer formation of AgBr and subsequent reduction [18]. The E_p value increases with increase of $1/m$ as shown in Fig. 9 where m is given by $(RT/F)(k_s/nv)$ [19]. The heterogenous rate constant (k_s) was calculated to be

Table 1. Analysis of current maxima for electrodeposition of AgBr on Ag

E (V vs NCE)	η (mV)	$10^3 i_m$ (A cm^{-2})	t_m (s)	$10^6 i_m^2 t_m$ (A^2 s cm^{-4})
−0.008	2	1.69	2.3	6.57
−0.006	4	1.79	2.05	6.57
−0.004	6	2.48	1.05	6.45
−0.002	8	3.04	0.70	6.47
−0.001	9	5.06	0.25	6.41

Table 2. Effect of sweep rate

Sweep rate, v (mV s^{-1})	*Peak potential* (V vs NCE)		*Peak potential difference* E_p (mV)
	anodic (E_{pa})	*cathodic* (E_{pc})	
11	−0.185	−0.185	0
30	−0.185	−0.185	0
40	−0.185	−0.185	0
50	−0.170	−0.200	30
100	−0.170	−0.210	40
180	−0.175	−0.220	55
270	−0.170	−0.245	75
400	−0.165	−0.235	70

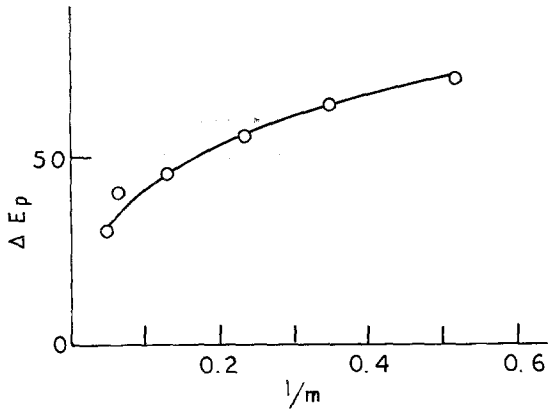

Fig. 9. Plot of ΔE_p vs $1/m$.

$30.03\,s^{-1}$ from the ΔE_p value of a and c, when $v_a = v_c = 0.1\,V\,s^{-1}$.

Single potential step current–time transients confirmed the diagnosis of adsorption-desorption kinetics in as much as they were monotonically falling.

References

[1] D. J. G. Ives and G. J. Janz, 'Reference Electrodes', Academic Press, New York (1961) p. 54.
[2] G. J. Moody and J. D. R. Thomas, 'Selective Ion Selective Electrodes', Merrow, Watford (1971).
[3] L. Slifkin, *Sci. Prog. Oxf.* **60** (1972) 151.
[4] L. J. Kurtz, *C.r. U.R.S.S.* **11** (1935) 383.
[5] W. Jaenicke, R. Tischer and H. Gerischer, *Z. Electrochem.* **59** (1955) 443.
[6] W. Jaenicke, *Z. Electrochem.* **55** (1951) 186.
[7] H. Lal, H. R. Thirsk and W. F. K. Wynne-Jones, *Trans. Faraday Soc.* **47** (1951) 70.
[8] V. I. Birss and G. S. Wright, *Electrochim. Acta* **27** (1982) 1429.
[9] S. Jaya, T. P. Rao and G. P. Rao, *Bull. Electrochem.* **2** (1986) 313.
[10] S. Jaya, T. P. Rao and G. P. Rao, *J. Appl. Electrochem.* (in press).
[11] S. Jaya, T. P. Rao and G. P. Rao, *J. Appl. Electrochem.* (in press).
[12] S. Fletcher, C. S. Halliday, D. Gates, M. Westcott, T. Lwin and G. Nelson, *J. Electroanal. Chem.* **159** (1983) 267.
[13] S. Fletcher, *Electrochim. Acta* **28** (1983) 917.
[14] G. T. Burstein and R. D. K. Misra, *Electrochim. Acta* **28** (1983) 363.
[15] D. A. Varmilyea, in 'Advances in Electrochemistry and Electrochemical Engineering' (edited by P. Delahay), Interscience, New York (1971) Vol. 3.
[16] S. Fletcher, *J. Chem. Soc. Faraday Trans. (I)* **79** (1983) 467.
[17] G. A. Gunawardena, G. J. Hills, I. Montenegro and B. R. Scharifker, *J. Electroanal. Chem.* **138** (1982) 225.
[18] E. Bosco and S. K. Rangarajan, *J. Electroanal. Chem.* **129** (1981) 25.
[19] E. Laviron, *J. Electroanal. Chem.* **101** (1979) 19.